

Universal conductance fluctuations and direct observation of crossover of symmetry classes in topological insulators

Saurav Islam¹, Semonti Bhattacharyya^{1,2}, Hariharan Nhalil¹, Suja Elizabeth¹, Arindam Ghosh^{1,3}

¹*Department of Physics, Indian Institute of Science, Bangalore: 560012.*

²*School of Physics and Astronomy, Monash University, VIC 3800, Australia. and*

³*Center for Nanoscience and Engineering, Indian Institute of Science, Bangalore: 560012.**

A key feature of disordered topological insulators (TI) is symplectic symmetry of the Hamiltonian which changes to unitary when time reversal symmetry is lifted and the topological phase transition occurs. However, such a crossover has never been explicitly observed, by directly probing the symmetry class of the Hamiltonian. In this report, we have probed the symmetry class of topological insulators by measuring the mesoscopic conductance fluctuations in the TI $\text{Bi}_{1.6}\text{Sb}_{0.4}\text{Te}_2\text{Se}$, which shows an exact factor of two reduction on application of a magnetic field due to crossover from symplectic to unitary symmetry classes. The reduction provides an unambiguous proof that the fluctuations arise from the universal conductance fluctuations (UCF), due to quantum interference and persists from $T \sim 22$ mK to 4.2 K. We have also compared the phase breaking length l_ϕ extracted from both magneto-conductivity and UCF which agree well within a factor of two in the entire temperature and gate voltage range. Our experiment confirms UCF as the major source of fluctuations in mesoscopic disordered topological insulators, and the intrinsic preservation of time reversal symmetry in these systems.

Topological insulators [1–4] at zero magnetic field are time reversal invariant systems characterized by surface states with a linear band structure. The Hamiltonian for such surface states is described by $H = \hbar v_F \vec{\sigma} \cdot \vec{k}$ which belongs to the AII/symplectic universality class, where v_F , $\vec{\sigma}$, and \vec{k} are the Fermi velocity, spin matrices, and momentum respectively. This is also known as the Anderson universality class for non-relativistic particles in the presence of a random spin-orbit coupling where time reversal symmetry (TRS) is preserved [5]. The addition of an external magnetic field or ferromagnetic impurities introduce a Zeeman/orbital term in the Hamiltonian and breaks the TRS which results in a topological to trivial phase transition in the bulk states and manifests as a gap opening in the linear surface states [3]. In terms of random matrix theory, this crossover at the surface states is well described by a crossover from AII/symplectic to A/unitary class in the system. Experimentally, the sensitivity of transport to magnetic impurities [6, 7] or the saturation of the phase breaking length at low temperatures are directly connected to the TRS in TI systems [8, 9]. This makes an explicit demonstration of the symplectic to unitary crossover an important task, which has however, not been achieved yet.

One direct method to probe such crossover of symmetry classes is universal conductance fluctuations (UCF) [10–12], which is observed in mesoscopic devices, when the length of the sample L becomes comparable to l_ϕ , the phase breaking length. UCF is an effect which results from quantum interference of all possible electron paths traversed between two points in a sample making the electrical conduction sensitive to the Fermi energy, magnetic field and impurity configuration. These fluctuations are

independent of the specific material properties or geometry, and is determined by the physical symmetries of the Hamiltonian. Within the framework of random matrix theory, the magnitude of UCF is proportional to [12]

$$\langle \delta G^2 \rangle \propto \left(\frac{e^2}{h} \right)^2 \frac{ks^2}{\beta} \quad (1)$$

Here β , s , and k are the Wigner-Dyson parameter, Kramer’s degeneracy, and the number of independent eigen modes of the Hamiltonian respectively (Table I). This UCF based technique has been previously used as an experimental probe in mesoscopic samples of graphene [13, 14], where a factor of four reduction was observed in the magnitude as a function of number density due to crossover from symplectic to orthogonal classes [15]. Similar reduction of noise with magnetic field were observed in metal films [16–19], metallic single crystals of silicon [20], and also in δ -doped silicon-phosphorous systems [21, 22]. Though a symmetry class crossover in TI has been induced by addition of ferromagnetic impurities and inferred from weak anti-localization [23], a more direct observation of the symmetry class and its crossover on breaking TRS, which does not require any addition of impurity remains experimentally elusive. In this report, we present results of conductance fluctuation measurements in topological insulator $\text{Bi}_{1.6}\text{Sb}_{0.4}\text{Te}_2\text{Se}$ on atomically thin hexagonal-boron nitride (hBN) substrate which shows a factor of two reduction on application of a magnetic field, thereby suggesting that the fluctuations indeed arise from UCF and the reduction is driven by a crossover from symplectic to unitary symmetry class. We have also extracted the phase breaking length from both magneto-conductance (l_ϕ^{MR}) and universal conductance fluctuations (l_ϕ^{UCF}) and found a close agreement.

The devices studied in this paper were fabricated from a 11 nm thick topological insulator $\text{Bi}_{1.6}\text{Sb}_{0.4}\text{Te}_2\text{Se}$ [24]

* isaurav@iisc.ac.in

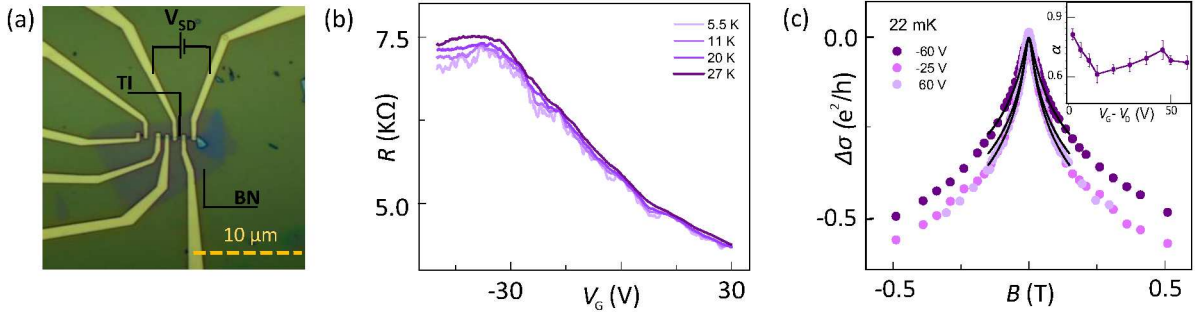


Figure 1. **Basic characteristics of TI field effect transistor (FET).** (a) Optical micrograph of a typical TI on BN FET device. (b) R - V_G of the device at different temperatures. (c) MR at three different gate voltages at $T = 22$ mK. The solid lines are fits to the data according to the Eq. 2 (inset shows α extracted from the fits using Eq. 2).

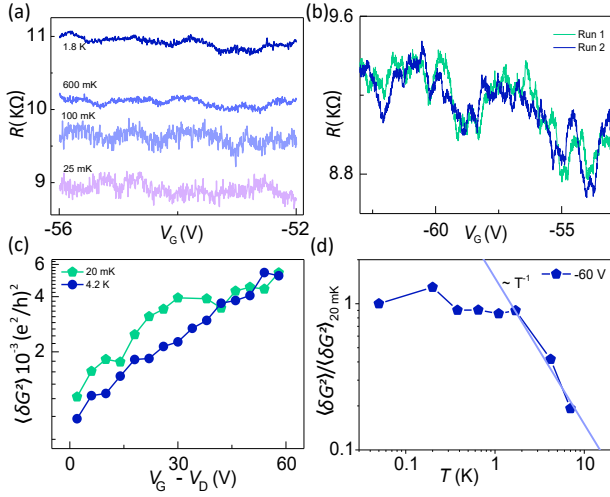


Figure 2. **Features of conductance fluctuations.** (a) R - V_G in a small gate voltage window of 4 V for four different temperatures used to calculate $\langle \delta G^2 \rangle$ by using a smooth polynomial fit. The curves have been offset for clarity. (b) R - V_G for two different runs showing the reproducibility of conductance fluctuations arising due to quantum interference. (c) Magnitude of conductance fluctuations as a function of gate voltage showing a monotonic increase away from the Dirac point. (d) T -dependence of $\langle \delta G^2 \rangle$ normalized by the magnitude at 20 mK showing a gradual decrease with increasing T , a characteristic feature of UCF. The solid line shows $\langle \delta G^2 \rangle \sim 1/T$ for $T > 2$ K.

exfoliated on SiO_2/Si wafer and then transferred onto a 14 nm hBN substrate. The heterostructure was then finally transferred onto a heavily doped SiO_2/Si substrate with the 285 nm thick SiO_2 acting as a back gate dielectric, using a home-made transfer technique. hBN was used to reduce the effect of dangling bonds and charged traps of the SiO_2 substrate on the electrical transport in the TI channel [25, 26]. The quaternary alloy $\text{Bi}_{1.6}\text{Sb}_{0.4}\text{Te}_2\text{Se}$ offers reduced bulk number density due to compensation doping resulting in enhanced surface transport [24]. The contact pads were defined by standard electron-beam lithography followed by metallization us-

Table I. Values of symmetry parameters for the two classes relevant for TI.

Ensemble	TRS	k	s	β	H_{ij}	$\langle \delta G^2 \rangle \propto \left(\frac{e^2}{h}\right)^2 \frac{k_s s^2}{\beta}$
Symplectic	Yes	1	2	4	real quaternion	1
Unitary	No	1	1	2	complex	0.5

ing 5/40 nm Cr/Au (Fig. 1(a)). The sample was coated with a layer of PMMA (poly(methylmethacrylate)) during the entire measurement cycle. All measurements from 22 mK to 4.2 K were done in a dilution refrigerator. Resistivity measurements were performed using a low frequency AC-four probe technique with carrier frequency of 18 Hz. The excitation current was 0.1 nA for most of the measurements to reduce the effect of Joule heating except at 4.2 K when it was increased to 1 nA. The resistance (R) vs gate voltage (V_G) is shown in Fig. 1(b), where a maximum in the resistance at $V_G \approx -38$ V at 5.5 K represents the Dirac point. The number density calculated at $V_G = 0$ V using $n = \frac{C_S(V_G - V_D)}{e}$ is $-2.9 \times 10^{16} \text{ m}^{-2}$. Here C_S is the series capacitance of SiO_2 and hBN layers. Fig. 1(c) shows weak-antilocalization phenomenon characterized by a cusp in the quantum correction to conductivity $\Delta\sigma$ at $B = 0$ T. Spin momentum locking in TI leads to an additional π Berry phase between the backscattered, time reversed path of the carriers, leading to negative magneto-conductance, a signature of the symplectic phase. The magneto-conductance data can be fitted with the Hikami-Larkin-Nagaoka (HLN) equation for diffusive metals with high spin orbit coupling ($\tau_\phi \gg \tau_{so}, \tau_e$) [9, 27]:

$$\Delta\sigma = -\alpha \frac{e^2}{\pi h} \left[\psi \left(\frac{1}{2} + \frac{B_\phi}{B} \right) - \ln \left(\frac{B_\phi}{B} \right) \right] \quad (2)$$

where τ_ϕ , τ_{so} , τ_e are the phase coherence or dephasing time, spin-orbit scattering time and elastic scattering time respectively, ψ is the digamma function and B_ϕ is the phase breaking field. Here α and B_ϕ are the fitting parameters. The phase coherence length (l_ϕ^{MR}) can

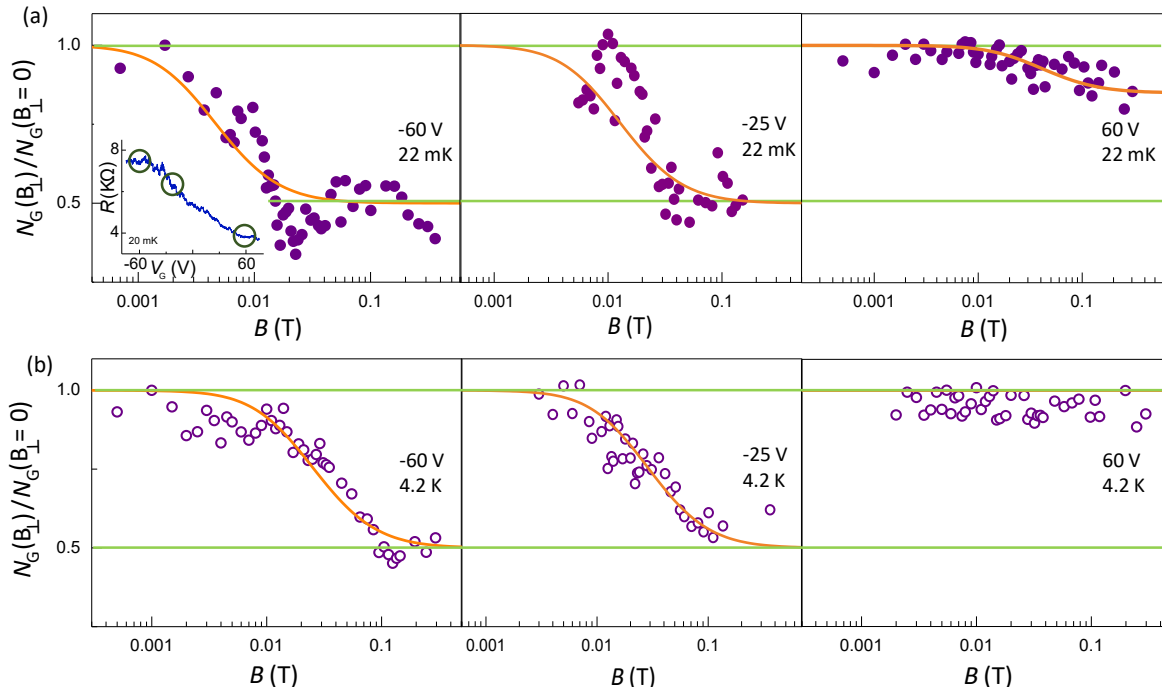


Figure 3. **Magnetic field dependence of normalized UCF magnitude.** (a) $v(B_{\perp}, T) = N_G(B_{\perp})/N_G(B_{\perp} = 0)$ for three different gate voltages (-60 V, -25 V and 60 V) for 22 mK clearly exhibiting a factor of two reduction which diminishes as the Fermi energy is tuned towards the bulk. The solid lines indicate fit to the data using Eq. 4. The noise data for 60 V at $T = 20$ mK has been fitted using the crossover function $v'(B, T)$ (See supplementary). Inset in (a) shows R vs V_G at $T = 20$ mK. The circled regions indicate windows where UCF was measured. (b) Normalized UCF magnitude three gate voltages -60 V, -25 V and 60 V at 4.2 K. The solid lines indicate fit to the data using Eq. 4.

be extracted using $l_{\phi}^{MR} = \sqrt{\hbar/4eB_{\phi}}$. The value of α gives an estimate of the number of independent conducting channels in the sample. $\alpha = 0.5$ indicates a single transport channel whereas a value of 1 indicates two independent channels contributing to magneto-transport. In our case, the value of α at $T = 22$ mK (inset of Fig. 1(c)) varies from 0.8 near the Dirac point ($V_G = -60$ V) and gradually reduces to a value of around 0.6 for more positive gate voltages. This probably indicates that as the Fermi energy is tuned away from the charge neutrality point, the bulk carriers start contributing to transport resulting in a reduction in the value of α , signifying coupling of bulk and surface transport [8].

The magnitude of conductance fluctuations $\langle \delta G^2 \rangle$, is evaluated using a method similar to Ref [15, 28] by varying the Fermi energy with the back gate voltage in steps of 5 mV over a small window of 4 V so that statistically meaningful data (about 800 realizations) are recorded, without changing the conductance appreciably in a two terminal configuration for each transverse magnetic field. $\langle \delta G^2 \rangle$ is extracted from R - V_G by fitting the data with a smooth polynomial curve [15, 28]. The variance of the residual of the fit gives the value of $\langle \delta R^2 \rangle$ and the mean value corresponds to $\langle R \rangle$. $\langle \delta G^2 \rangle$ is then obtained using the relation: $\langle \delta G^2 \rangle = \langle \delta R^2 \rangle / \langle R \rangle^4$.

Fig. 2(a) shows typical R - V_G sweeps at four different temperatures for the device, where the fluctuations decrease with T , a hallmark of UCF. The run to run reproducibility as a function of V_G in Fig. 2(b) further confirms the aperiodic yet reproducible nature of the fluctuations. The V_G -dependence of $\langle \delta G^2 \rangle$ is shown in Fig 2(c). The magnitude of $\langle \delta G^2 \rangle$ shows an increase as the Fermi energy is tuned away from the electron-hole puddle dominated regime towards higher number densities. Such behavior is a unique signature of Dirac Fermionic systems like TI surface states where the disorder potential due to charged impurities is long range in nature [15, 29]. At more positive gate voltages, the value of $\langle \delta G^2 \rangle$ at $T = 20$ mK and 4.2 K are similar. This may be due to increased contribution of scattering due to bulk defects which are the dominant source of noise in TI [30–34]. The temperature dependence of conductance fluctuations (Fig. 2(d)), shows an increase as T is reduced to 2 K, below which it saturates. The saturation of $\langle \delta G^2 \rangle$ at $T < 2$ K can be due to saturation of l_{ϕ} . Such saturation has been previously seen in various systems and can arise due to the presence of magnetic impurities in the system [35] or when the spin orbit length becomes comparable to the phase breaking length [36]. For $T > 2$ K, the magnitude of $\langle \delta G^2 \rangle$ decreases with increasing T as $\langle \delta G^2 \rangle \propto 1/T$ which

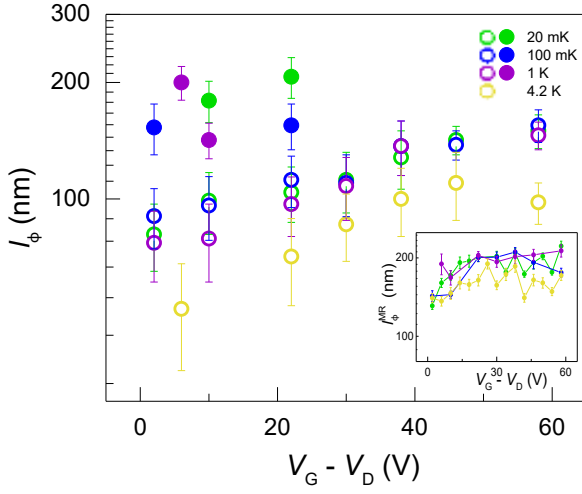


Figure 4. **Comparison of phase breaking length (l_ϕ) from different methods.** l_ϕ extracted from UCF as a function of V_G for different T from magnetic field dependence using Eq. 4 (solid circles) and directly at $B_\perp = 0$ T using Eq. 5 (hollow circles). Inset shows l_ϕ^{MR} extracted from magneto-conductance using Eq. 2 as a function of V_G for different T . l_ϕ obtained from three different methods agree well within a factor of two.

can be explained from the dependence of $\langle \delta G^2 \rangle$ on l_ϕ and the number of active fluctuators (n_s). For $T \rightarrow 0$, UCF magnitude $\langle (\delta G^2)^2 \rangle^{\frac{1}{2}} \rightarrow e^2/h$, while at finite temperature [11, 18, 21],

$$\langle \delta G^2 \rangle \simeq \left(\frac{e^2}{h} \right)^2 \alpha(k_F \delta r) \frac{1}{k_F l} \frac{L_y}{L_x^3} n_s(T) l_\phi^4 \quad (3)$$

where k_F , l , L_x and L_y are the Fermi wave-vector, mean free path and sample dimensions in x and y directions respectively. $\alpha(x)$ represents the change of the phase of electron wave-function due to scattering by a moving impurity at a distance δr . Assuming electron-electron interaction mediated dephasing, $l_\phi^2 \propto 1/T$ and $n_s(T) \propto T$ [11, 18, 21, 37], we have $\langle \delta G^2 \rangle \propto l_\phi^4 n_s(T) \propto 1/T$ (Fig. 2(d)), as observed at $T > 2$ K.

In order to (a) conclusively establish the role of UCF, and (b) investigate the crossover in the symmetry class directly, we have measured $\langle \delta G^2 \rangle$ as a function of perpendicular magnetic field (B_\perp) at fixed V_G . The magnitude of the conductance fluctuations is plotted as $v(B_\perp, T) = N_G(B_\perp)/N_G(B_\perp = 0)$ where $N_G = \langle \delta G^2 \rangle / \langle G^2 \rangle$ is the normalized variance. As a function of increasing B_\perp , as shown in Fig. 3(a) and Fig. 3(b) at $T = 22$ mK and $T = 4.2$ K, we observe a clear factor of two reduction in the UCF magnitude at -60 V and -25 V whereas at 60 V, the reduction significantly reduced. For gate voltages closer to the Dirac Point (-60 V and -25 V), the reduction occurs for $B_\perp \sim 0.01 - 0.1$ T, which is similar to the field scales for quantum interference effect (B_ϕ)

reported for TI [8, 38]. Since $B_\phi \sim \hbar/4el_\phi^2$, the increase in field scales with T can be readily attributed to the decrease in l_ϕ with increasing T . Although $l_\phi \propto T^{-1/2}$ expected from electron-electron scattering would lead to much larger change in B_ϕ in the experimental temperature range, we believe a saturation in l_ϕ [35, 36] limits the decrease in B_ϕ at low temperatures. The absence of a clear reduction by a factor of two at high positive voltages can be due to additional noise contributions in the system. As E_F is tuned towards the bulk bands, trapping-detrapping processes from the charged impurities in the bulk, which are independent of B_\perp , and are known to be dominant source of noise in TI increases [30–34], which diminishes the factor of two reduction.

For a quantitative understanding, we have fitted the normalized magnitude with the expression [21, 39, 40]

$$v(B, T) = \frac{1}{2} + \frac{1}{b^2} \sum_{n=0}^{\infty} \frac{1}{[(n + \frac{1}{2}) + \frac{1}{b}]^3} \\ = \frac{1}{2} - \Psi'' \frac{1}{2b^2} \left(\frac{1}{2} + \frac{1}{b} \right) \quad (4)$$

Here $b = 8\pi B(l_\phi)^2/(h/e)$ and Ψ'' is the double derivative of the digamma function and l_ϕ is the fitting parameter. The solid lines in Fig. 3 are fits according to Eq. 4, which capture the variation of noise magnitude with B_\perp well, especially at gate voltage values close to the Dirac point. The corresponding l_ϕ , extracted from fitted value of b , are plotted in Fig. 4 (solid circles). At $V_G = 60$ V, the overall reduction allows us to estimate ≈ 28 % of the observed noise magnitude to arise from UCF at $T = 20$ mK (Fig. 3(a)) but becomes negligibly small at higher T (Fig. 3(b)).

Finally, we have evaluated the V_G -dependence of l_ϕ from three different methods (a) $\langle \delta G^2 \rangle$ magnitude, (b) B_\perp -dependence of noise, and (c) magneto-conductance. We have however, restricted the calculation between $V_G = -60$ V to 0 V, where UCF is the dominant source of noise. l_ϕ extracted directly from $\langle \delta G^2 \rangle$ at $B_\perp = 0$ T using the expression [5, 41, 42]:

$$\langle \delta G^2 \rangle \simeq \frac{3}{\pi} \left(\frac{e^2}{h} \right)^2 \left(\frac{l_\phi}{L} \right)^2 \quad (5)$$

is shown in Fig. 4 ($L = W$ (width) = $2 \mu\text{m}$) (hollow circles), while l_ϕ^{MR} extracted from magneto-conductance using Eq. 2, is shown in the inset of Fig. 4. We find that l_ϕ^{MR} and l_ϕ^{UCF} (obtained from both Eq. 4 and Eq. 5) are similar in magnitude within a factor of two, rendering validity to the factor of two reduction and the corresponding analysis. l_ϕ^{MR} increases away from the Dirac point, similar to the trend of l_ϕ obtained from UCF (Fig. 4). Near the Dirac point, the system is highly inhomogeneous with the presence of electron-hole puddles. As the gate voltages is tuned away from the charge neutrality point, the carrier concentration increases leading to enhanced

screening which suppresses dephasing due to electromagnetic fluctuations. This leads to a larger phase breaking length away from the Dirac point [43–45]. The factor of two difference in l_ϕ obtained from magneto-conductance and magneto-noise can arise because Eq. 5 is valid in the case of $L_\phi \ll L, L_T$ [5, 42], where L_T is the thermal length. Moreover, the phase breaking time τ_ϕ and hence, the phase breaking length $l_\phi = \sqrt{D\tau_\phi}$ (D is the electron diffusivity) relevant for weak localization (WL) is related to the Nyquist dephasing rate [37], whereas in case of UCF, the relevant scattering time for 2D is the out-scattering time maybe related to the inverse of the inelastic collision frequency and differ by a logarithmic

factor compared to the WL rate [16, 21, 46–49].

In conclusion, we have measured the Fermi energy dependent aperiodic and reproducible fluctuations in mesoscopic topological insulator systems. The magnetic field dependence of these fluctuations conclusively indicate that they arise from universal conductance fluctuations. Most importantly, a factor of two reduction in noise magnitude close to the Dirac point is observed, which provides an unambiguous proof that the time reversal symmetry in disordered topological insulators is intrinsically maintained.

We thank Saquib Shamim for useful discussions. We acknowledge the Department of Science and Technology (DST) for funding.

-
- [1] M. Z. Hasan and C. L. Kane, *Rev. Mod. Phys.*, **82**, 3045 (2010).
- [2] J. E. Moore, *Nature*, **464**, 194 (2010).
- [3] B. A. Bernevig, T. L. Hughes, and S.-C. Zhang, *Science*, **314**, 1757 (2006).
- [4] M. König, S. Wiedmann, C. Brüne, A. Roth, H. Buhmann, L. W. Molenkamp, X.-L. Qi, and S.-C. Zhang, *Science*, **318**, 766 (2007).
- [5] P. Adroguer, D. Carpentier, J. Cayssol, and E. Orignac, *New J. Phys.*, **14**, 103027 (2012).
- [6] C.-Z. Chang, J. Zhang, X. Feng, J. Shen, Z. Zhang, M. Guo, K. Li, Y. Ou, P. Wei, L.-L. Wang, *et al.*, *Science*, 1232003 (2013).
- [7] L. Bao, W. Wang, N. Meyer, Y. Liu, C. Zhang, K. Wang, P. Ai, and F. Xiu, *Sci. Rep.*, **3**, 2391 (2013).
- [8] J. Liao, Y. Ou, H. Liu, K. He, X. Ma, Q.-K. Xue, and Y. Li, *Nat. Comm.*, **8**, 16071 (2017).
- [9] L. Bao, L. He, N. Meyer, X. Kou, P. Zhang, Z.-g. Chen, A. V. Fedorov, J. Zou, T. M. Riedemann, T. A. Lograsso, *et al.*, *Sci. Rep.*, **2**, 726 (2012).
- [10] P. A. Lee and A. D. Stone, *Phys. Rev. Lett.*, **55**, 1622 (1985).
- [11] S. Feng, P. A. Lee, and A. D. Stone, *Phys. Rev. Lett.*, **56**, 1960 (1986).
- [12] B. Altshuler and B. Shklovskii, *Zh. Eksp. Teor. Fiz.*, **91**, 220 (1986).
- [13] K. S. Novoselov, A. K. Geim, S. V. Morozov, D. Jiang, Y. Zhang, S. V. Dubonos, I. V. Grigorieva, and A. A. Firsov, *Science*, **306**, 666 (2004).
- [14] A. C. Neto, F. Guinea, N. M. Peres, K. S. Novoselov, and A. K. Geim, *Rev. Mod. Phys.*, **81**, 109 (2009).
- [15] A. N. Pal, V. Kochat, and A. Ghosh, *Phys. Rev. Lett.*, **109**, 196601 (2012).
- [16] P. McConville and N. O. Birge, *Phys. Rev. B*, **47**, 16667 (1993).
- [17] N. O. Birge, B. Golding, and W. Haemmerle, *Phys. Rev. Lett.*, **62**, 195 (1989).
- [18] N. O. Birge, B. Golding, and W. Haemmerle, *Phys. Rev. B*, **42**, 2735 (1990).
- [19] J. Moon, N. O. Birge, and B. Golding, *Phys. Rev. B*, **53**, R4193 (1996).
- [20] A. Ghosh and A. Raychaudhuri, *Phys. Rev. Lett.*, **84**, 4681 (2000).
- [21] S. Shamim, S. Mahapatra, G. Scappucci, W. Klesse, M. Simmons, and A. Ghosh, *Sci. Rep.*, **7** (2017).
- [22] S. Shamim, S. Mahapatra, G. Scappucci, W. Klesse, M. Simmons, and A. Ghosh, *Phys. Rev. Lett.*, **112**, 236602 (2014).
- [23] H.-T. He, G. Wang, T. Zhang, I.-K. Sou, G. K. Wong, J.-N. Wang, H.-Z. Lu, S.-Q. Shen, and F.-C. Zhang, *Phys. Rev. Lett.*, **106**, 166805 (2011).
- [24] A. Taskin, Z. Ren, S. Sasaki, K. Segawa, and Y. Ando, *Phys. Rev. Lett.*, **107**, 016801 (2011).
- [25] C. R. Dean, A. F. Young, I. Meric, C. Lee, L. Wang, S. Sorgenfrei, K. Watanabe, T. Taniguchi, P. Kim, K. L. Shepard, *et al.*, *Nat. Nanotechnol.*, **5**, 722 (2010).
- [26] P. Karnatak, T. P. Sai, S. Goswami, S. Ghatak, S. Kaushal, and A. Ghosh, *Nat. Comm.*, **7**, 13703 (2016).
- [27] S. Hikami, A. I. Larkin, and Y. Nagaoka, *Prog. Theor. Phys.*, **63**, 707 (1980).
- [28] R. Gorbachev, F. Tikhonenko, A. Mayorov, D. Horsell, and A. Savchenko, *Phys. Rev. Lett.*, **98**, 176805 (2007).
- [29] E. Rossi, J. Bardarson, M. Fuhrer, and S. DasSarma, *Phys. Rev. Lett.*, **109**, 096801 (2012).
- [30] S. Bhattacharyya, M. Banerjee, H. Nhalil, S. Islam, C. Dasgupta, S. Elizabeth, and A. Ghosh, *ACS Nano*, **9**, 12529 (2015).
- [31] S. Bhattacharyya, A. Kandala, A. Richardella, S. Islam, N. Samarth, and A. Ghosh, *Appl. Phys. Lett.*, **108**, 082101 (2016).
- [32] S. Islam, S. Bhattacharyya, A. Kandala, A. Richardella, N. Samarth, and A. Ghosh, *Appl. Phys. Lett.*, **111**, 062107 (2017).
- [33] J. Pelz and J. Clarke, *Phys. Rev. B*, **36**, 4479 (1987).
- [34] S. Hershfield, *Phys. Rev. B*, **37**, 8557 (1988).
- [35] F. Schopfer, C. Bäuerle, W. Rabaud, and L. Saminadayar, *Phys. Rev. Lett.*, **90**, 056801 (2003).
- [36] Y. K. Fukai, S. Yamada, and H. Nakano, *Appl. Phys. Lett.*, **56**, 2123 (1990).
- [37] B. L. Altshuler, A. Aronov, and D. Khmelnitsky, *J. Phys. C: Solid State Phys.*, **15**, 7367 (1982).
- [38] S. Zhang, R. McDonald, A. Shekhter, Z. Bi, Y. Li, Q. Jia, and S. T. Picraux, *Appl. Phys. Lett.*, **101**, 202403 (2012).
- [39] A. D. Stone, *Phys. Rev. B*, **39**, 10736 (1989).
- [40] P. Lee, A. D. Stone, and H. Fukuyama, *Phys. Rev. B*, **35**, 1039 (1987).
- [41] C. Beenakker and H. van Houten, in *Solid State Phys.*, Vol. 44 (Elsevier, 1991) pp. 1–228.

- [42] E. Akkermans and G. Montambaux, *Mesoscopic physics of electrons and photons* (Cambridge University Press, 2007).
- [43] J. Tian, C. Chang, H. Cao, K. He, X. Ma, Q. Xue, and Y. P. Chen, *Sci. Rep.*, **4** (2014).
- [44] S.-P. Chiu and J.-J. Lin, *Phys. Rev. B*, **87**, 035122 (2013).
- [45] J. Martin, N. Akerman, G. Ulbricht, T. Lohmann, J. v. Smet, K. Von Klitzing, and A. Yacoby, *Nat. Phys.*, **4**, 144 (2008).
- [46] Y. M. Blanter, *Phys. Rev. B*, **54**, 12807 (1996).
- [47] D. Hoadley, P. McConville, and N. O. Birge, *Phys. Rev. B*, **60**, 5617 (1999).
- [48] A. Trionfi, S. Lee, and D. Natelson, *Phys. Rev. B*, **70**, 041304 (2004).
- [49] V. Chandrasekhar, P. Santhanam, and j. v. n. p. y. p. Prober, D.E.,.